Available online at www.sciencedirect.com
SCIENCE DIRECT®
Electrochimica Acta 49 (2004) 4149–4156
ELECTROCHIMICA Acta
www.elsevier.com/locate/electacta

Effects of hydrophobic polymer content in GDL on power performance of a PEM fuel cell

Chan Lim[1], C.Y. Wang*

Department of Materials Science and Engineering, Electrochemical Engine Center (ECEC), The Pennsylvania State University, University Park, PA 1680, USA

Received 1 April 2004; received in revised form 11 April 2004; accepted 12 April 2004

Available online 14 May 2004

Abstract

Effects of hydrophobic polymer content within a carbon paper, used as the cathode gas diffusion layer (GDL), on power performance of a H_2/air proton exchange membrane fuel cell (PEMFC) have been studied. Electrochemical methods are used in conjunction with morphology and wetting property characterization. Surface contact angle of wet-proof-treated GDL as a function of temperature is measured by a novel capillary rise method. It is shown that the contact angle generally decreases with the temperature, and that there is insignificant difference in contact angle on carbon papers treated with different contents of fluorinated ethylene propylene (FEP) ranging from 10 to 40 wt.%. Under all humidification conditions in this study, a membrane-electrode assembly (MEA) consisting of 10 wt.% FEP-impregnated GDL shows higher power densities than 30 wt.% FEP-impregnated one. Surface morphology of the hydrophobic polymer-treated carbon paper has been analyzed by scanning electron microscopy (SEM) and is identified as playing a crucial role in affecting the power performance of such treated GDL in the PEM fuel cell.

Keywords: Polymer electrolyte fuel cells; Gas diffusion layer; Hydrophobic polymer; Porosity; Power density

1. Introduction

In order to make fuel cell technology cost-competitive to conventional energy-conversion technologies, much research has been focused on fabricating high-power membrane-electrode assembly (MEA) that maximizes catalyst utilization at ultra-low loading of precious metal. To date, most of catalyst layers for hydrogen- or reformate gas-fed proton exchange membrane fuel cells (PEMFC) operated in the temperature range from room temperature up to 90 °C are fabricated by mixing Nafion® ionomer solution with Pt or Pt alloy catalyst supported on carbon black as suggested by Wilson and co-workers [1–3].

In the MEA, the catalyst layer is usually supported on a gas diffusion layer (GDL) that is made of either a woven carbon cloth or a non-woven carbon paper due to their high porosity and electric conductivity. Although the MEA based upon carbon cloth may present higher power performance than that of carbon paper [4–6], there are considerable academic and industrial interests in using carbon paper as there is a cost advantage with non-woven substrate and it is more convenient to fabricate a micro-porous layer (MPL) or catalyst layer directly onto it. Prior research has been performed to understand the role of MPL generally consisting of carbon black and polytetrafluoroethylene (PTFE) [7], and to optimize the PTFE content in MPL [8] and pore structure of MPL with various types of carbon blacks [9–11].

The MPL, placed between the catalyst layer and GDL, is intended to provide wicking of liquid water into the GDL, minimize electric contact resistance with the adjacent catalyst layer, and furthermore prevent the catalyst layer ink from leaking into the GDL, thereby increasing the catalyst utilization and reducing the tendency of electrode flooding. Much work in literature has thus focused on how to optimize the MPL morphologically, compositionally and dimensionally for better water management and higher catalyst utilization. However, less attention has been paid to the optimization of

* Corresponding author. Tel.: +1-814-863-4762; fax: +1-814-863-4848.
E-mail address: cxw31@psu.edu (C.Y. Wang).
[1] Present address: Department of Chemical Engineering and Advanced Materials, University of Newcastle upon Tyne, NE17RU Newcastle, UK.

0013-4686/$ – see front matter © 2004 Elsevier Ltd. All rights reserved.
doi:10.1016/j.electacta.2004.04.009

GDL, i.e. an optimal fluorinated ethylene propylene (FEP) content. In the present study, effects of the FEP content in the carbon paper GDL are investigated without interposing MPL between the catalyst layer and carbon paper GDL to avoid possible ambiguities from the presence of MPL.

2. Experimental

Both an anode and a cathode consisted of a wet-proofed carbon paper and a catalyst layer. Commercial carbon papers (Toray 090, E-Tek) were made hydrophobic by treating with fluorinated ethylene propylene (FEP-60, Electrochem. Inc.) as follows [12–14]. To remove dusts inside the carbon paper (30 cm × 30 cm), it was rinsed in an acetone solution and then dried at 80 °C. The carbon paper was slowly dipped into a FEP suspension, diluted to 20 wt.% with de-ionized water, and then was dried at 80 °C by placing it over nine pins (diameter 2 mm), attached to a plate inside an oven, in order to achieve uniform distribution of FEP polymer inside the carbon paper. The procedure was repeated until desired weight gains, FEP content of 10 or 30 wt.%, are achieved. The FEP-impregnated carbon paper was heat-treated at 270 °C for 10 min. to remove a surfactant originating from the FEP emulsion and then finally sintered at 340 °C for 30 min. The FEP-impregnated carbon paper was directly used as a cathode GDL. In case of MPL-coated cathode GDL, the layer was fabricated on a 30 wt.% FEP-impregnated GDL by the tape-casting method [15]. The 30 wt.% FEP-impregnated carbon paper was also employed as the anode GDL for all MEAs tested in this work.

A commercial 5 wt.% Nafion solution (EW1100, Aldrich) was treated with diluted sodium hydroxide solution, resulting in Na^+ form of the Nafion solution. Subsequently, the Nafion solution was modified by adding a polar organic solvent (e.g. ethylene glycol) having higher viscosity than the Nafion solution consisting of aliphatic alcohols and water. A slurry for the catalyst layer was prepared by dispersing carbon-supported 20 wt.% Pt/C (E-Tek Inc.) powder into the modified Nafion solution, followed by mixing those with Agate pestle and mortar. The resultant slurry was directly spread onto the FEP-impregnated carbon paper by using a knife-blade, cured at 160 °C for 30 min. in an inert atmospheric oven, re-protonated to H^+ form of Nafion in a diluted sulfuric acid solution and then dried again in an oven at 80 °C for 1 h. The resulting amount of Pt and Nafion loading was 0.22 and 0.42 mg/cm^2, respectively, on both electrodes.

A commercial Nafion 112 membrane (EW 1100, Dupont) was treated according to a well-known membrane cleaning procedure [16]. After trimming the catalyzed electrodes for the anode and cathode respectively, they were positioned on both sides of the pre-cleaned Nafion 112 and hot-pressed to form a unit of MEA at 125 °C and 100 kgf/cm^2 for 3 min. The MEA was immersed into water at least overnight before installing into a single cell fixture (active area of 25 cm^2 with gold-coated Ti current collector plates, LynnTech. Inc.), having two-pass serpentine flow channels of the width and depth of 1 and 0.8 mm, respectively.

The single cell fixture, including membrane-electrode assembly, was connected to an in-house fuel cell test station and fed with humidified H_2/air on anode and cathode at constant flow rates. The flow rate of hydrogen was kept constant at a stoichiometry of 1.7 calculated at 1 A/cm^2, while the flow rate of air was varied. The anode and cathode gases were humidified by flowing through bubbler-type humidifiers heated at prescribed temperatures. The anode and cathode inlet temperatures were controlled to be the same as their humidification temperatures. The single cell was pressurized to a gauge pressure of 30 psi on both anode and cathode sides. Polarization curves were obtained using an Arbin BT + 4 testing system in a galvano-dynamic polarization mode at a scan rate of 2 mA/s. Cell ohmic resistances were obtained at a frequency of 1.5 kHz using a Solartron 1287

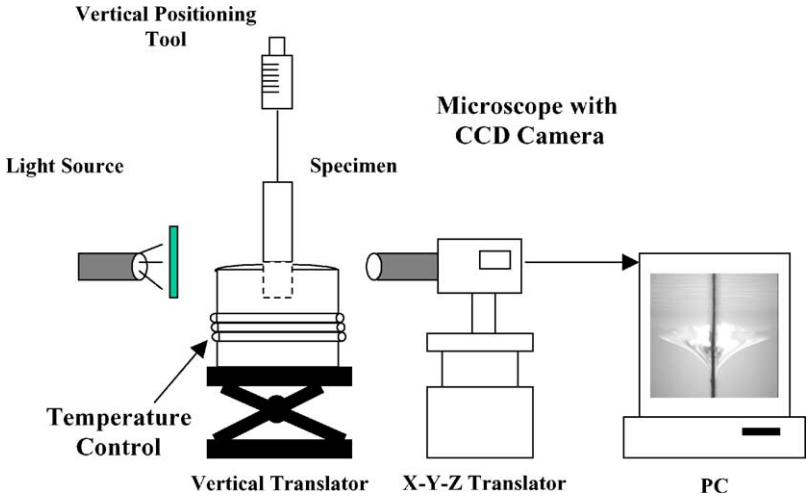

Fig. 1. Schematic of the experimental set-up for contact angle measurements.

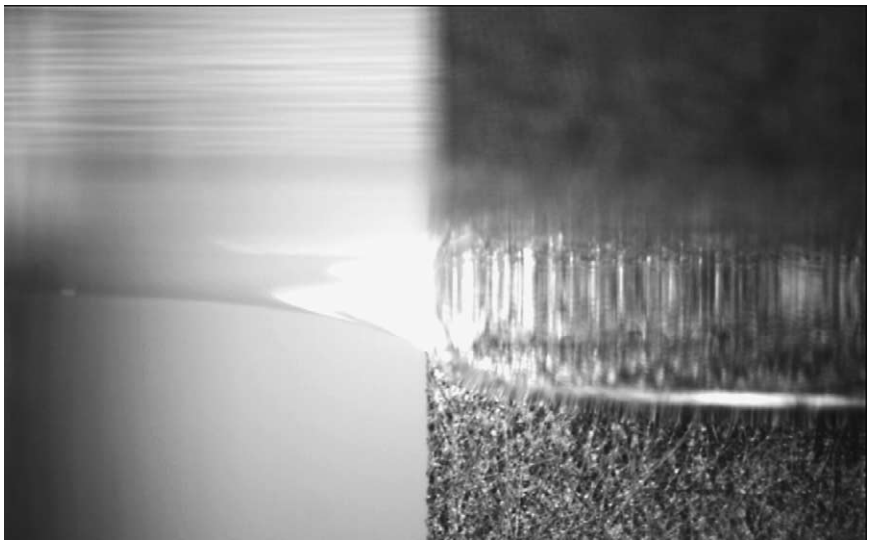

Fig. 2. Typical image of the meniscus line on the surface of a wet-proofed carbon paper in water pool.

Electrochemical Interface in conjunction with a Solartron 1260 Frequency Response Analyzer.

To characterize the GDL surface wetting properties, i.e. water contact angle or GDL hydrophobicity, we adapted a capillary rise method originally developed by Neumann and co-workers [17,18]. While the traditional capillary rise method is based on Wilhelmy plate gravimetric technique, the present method is modified to use an optical technique to directly record and measure the capillary meniscus height. Considering the force balance between gravity and surface tension through a meniscus line, the contact angle between liquid and the substrate specimen has the following relationship with the meniscus height [17]:

$$\sin\theta = 1 - \frac{\Delta\rho g h^2}{2\sigma} \tag{1}$$

where θ is the contact angle, $\Delta\rho$ the difference between the densities of liquid and vapor, g the gravitational acceleration, h the meniscus height, and σ the liquid–gas surface tension of water. Therefore, the contact angle can be calculated from a meniscus height measured experimentally. The schematic of the experimental set-up for the meniscus measurement is shown in Fig. 1.

After a specimen is dipped into a heated water pool by using a micrometer-driven horizontal translator, the meniscus height was measured by a microscope positioned on a X–Y–Z metric stage and connected to a television monitor via a charge coupled device (CCD) camera. Contact angles between water and GDL were determined by measuring meniscus heights from the initial unperturbed water level to an interfacial line between water, specimen and air, as shown in Fig. 2. If the specimen has a hydrophobic surface, a negative meniscus height, which is lower than the water pool level, will appear on the GDL surface. On the other hand, if the specimen is hydrophilic, a positive meniscus height, which is higher than the water pool level, will be observed.

The present method works for GDL with asymmetric wetting properties on two surfaces as commonly encountered in fuel cell applications, where a MPL may be placed on one side. In contrast, the traditional Wilhelmy plate gravimetric technique would require two different tests to quantify the differing wettability on two surfaces. Another common technique to characterize contact angles is sessile drop method which involves placing a small water droplet on the GDL substrate. Temperature control becomes difficult in this method as the temperature of the tiny water droplet quickly decreases as it falls from the syringe onto the GDL substrate.

3. Results and discussion

Liquid water transport through GDL and ensuing flooding relies strongly on not only pore structure, porosity and permeability but also degree of hydrophobicity or contact angle, as discussed in detail by Wang [19], and Pasaogullari and Wang [20]. Therefore, advancing and receding meniscus

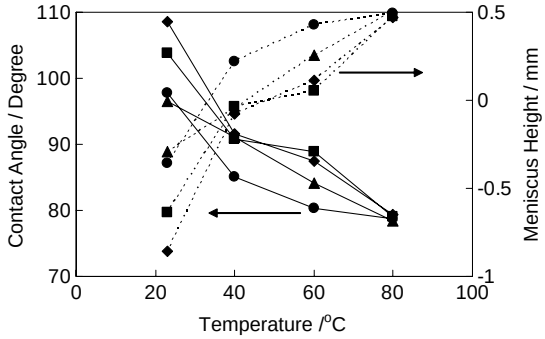

Fig. 3. Mean meniscus height and contact angle vs. temperature of meniscus pool obtained from capillary height measurements on carbon paper containing different amounts of FEP: (●) 10 wt.%; (■) 20 wt.%; (▲) 30 wt.%; (◆) 40 wt.% FEP-treated GDL.

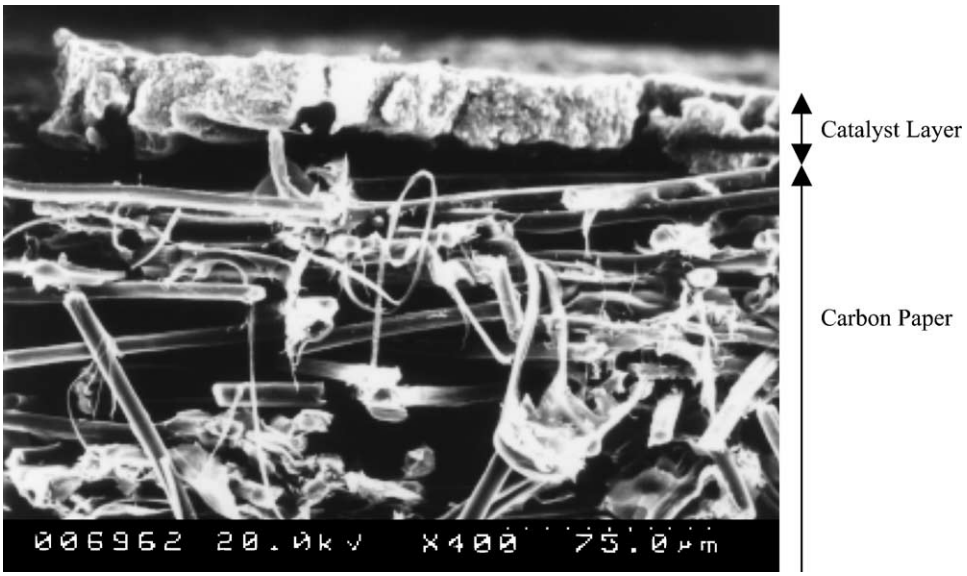

Fig. 4. Cross-sectional SEM micrograph of the interfacial region between the catalyst layer and carbon paper GDL.

heights as a function of temperature of the water pool were measured on various carbon papers with FEP contents of 10, 20, 30, 40 wt.%. The advancing and receding meniscus heights were evaluated three times at each temperature, and their mean value was used to calculate the contact angle by Eq. (1) and the results are shown in Fig. 3 as a function of temperature of meniscus pool. No systematic variations in contact angle are seen in Fig. 3 among all GDL samples with different FEP contents, implying that impregnation of 10 wt.% FEP into the carbon paper is probably sufficient to coat surfaces of carbon fibers constituting the carbon paper GDL. Further increase in FEP content would only thicken the FEP coating layer without changing the surface hydrophobicity appreciably. However, it is clearly observed in Fig. 3 that the contact angles of carbon papers treated with 10–40 wt.% FEP rapidly decreased from the range of 98–108° to 80° as the temperature of water pool was increased from 25 to 80 °C.

A cross-section of the catalyst layer/GDL interface was taken by scanning electron microscopy (SEM) and is presented in Fig. 4. As the slurry of the catalyst layer was prepared using the modified Nafion solution of high viscosity, we could minimize the penetration of the catalysts into the carbon paper after applying the slurry on it. As a result, the catalyst layer is shown in Fig. 4 to have a uniform thickness of 25 μm approximately on the wet-proofed carbon paper. Graphite fibers intermixed with FEP are seen below the catalyst layer, forming the non-woven carbon paper GDL substrate.

To investigate effects of hydrophobic polymer in a cathode GDL on polarization characteristics of a single cell, MEAs were fabricated in-house with three different types of cathode GDL. One was based on 10 wt.% FEP-impregnated carbon paper as the cathode GDL. Another was with 30 wt.% FEP-impregnated carbon paper. The last one was with 30 wt.% FEP-impregnated carbon paper plus a microporous layer (MPL, 40 wt.% PTFE + Vulcan carbon black, carbon loading of 1.5 mg/cm^2). While the first two types of GDL without MPL enables a fundamental study of the roles played by GDL, the third MEA shows the effects of adding MPL, a common practice widely adopted in the industry.

Fig. 5 shows the effect of three different cathode GDLs on the polarization behaviors of MEAs obtained at a cell temperature of 80 °C under hydrogen and air humidified at 95 and 90 °C, respectively. In this operating condition, the cathode is expected to be in an over-saturated environment. The MEA made of 10 wt.% FEP-impregnated cathode GDL showed a current density of 800 mA/cm^2 at 0.6 V at an air stoichiometry of 2.1, whereas the MEAs of 30 wt.% FEP-impregnated cathode GDL with and without MPL recorded current densities of 330 and 440 mA/cm^2,

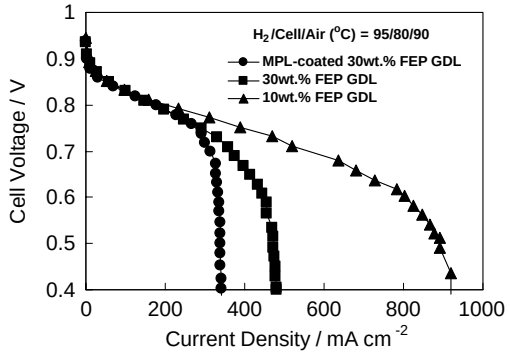

Fig. 5. Polarization curves obtained at 80 °C in 30 psi H_2/air from MEAs with three different types of cathode GDL under an air stoichiometry of 2.1 (@ 1 A/cm^2 equivalent): (●) microporous layer-coated and 30 wt.% FEP-impregnated cathode GDL; (■) 30 wt.% FEP-impregnated cathode GDL; (▲) 10 wt.% FEP-impregnated cathode GDL. Anode and cathode humidification temperature was 95 and 90 °C, respectively. Pt loading was 0.22 mg/cm^2 on both electrodes.

respectively, at 0.6 V, i.e. only about 40 and 55% compared to that of 10 wt.% FEP-impregnated cathode GDL. As seen in Fig. 5, the MEA based on 30 wt.% FEP-treated cathode GDL has very similar performance in the kinetic regime to that of MPL-coated 30 wt.% FEP GDL under well-humidified gas feed. However, at higher current densities it appears that MPL imposes an additional diffusion resistance to oxygen transport into the catalyst layer, making the mass transport limiting current smaller. However, note that, when properly designed and fabricated, MPL should be also beneficial at high current densities.

In the over-humidified environment on the cathode, the porous GDL is likely flooded, i.e. filled up with liquid water. Thus, one would expect that more hydrophobic GDL would have a less degree of flooding in the GDL and hence a higher mass transport limiting current. While the result of contact angle measurements displayed in Fig. 3 shows similar hydrophobicity between the 10 and 30 wt.% FEP-treated GDLs, Fig. 5 indicates that the 10 wt.% FEP-treated GDL yields a higher mass transport limiting current density. We shall provide a possible explanation for these seemingly contradictory results later in this section.

Fig. 6 shows the effect of air flow rate on the polarization behavior of MEAs with two different FEP-treated cathode GDLs at a cell temperature of 80 °C under hydrogen and air humidified at 95 and 90 °C, respectively. The limiting current density of the MEA with 30 wt.% FEP-impregnated cathode GDL increased merely by 30 mA/cm^2 as the air flow rate was increased from 2.1 to 4; on the other hand, that of 10 wt.% FEP-impregnated GDL increased by 130 mA/cm^2 as the air flow rate was increased. Clearly the MEA using 10 wt.% FEP-impregnated cathode GDL exhibits a higher sensitivity to the air flow rate than the 30 wt.% FEP-impregnated GDL, indicating that the latter is likely more flooded with liquid water than the former.

Fig. 7 displays polarization curves obtained at the cell temperature of 90 °C from MEAs of 30 and 10 wt.% FEP-impregnated cathode GDL under air stoichiometries of 2.1 and 4. The humidifier temperature of hydrogen and air was 95 and 80 °C, respectively, providing a slightly under-humidified environment in the cathode side. The MEA with 10 wt.% FEP-impregnated cathode showed a current density of 1040 mA/cm^2 at 0.6 V and air stoichiometry of 2.1, while the MEA of 30 wt.% FEP-impregnated GDL showed a current density of 940 mA/cm^2, i.e. 90% compared to that of 10 wt.% FEP-impregnated GDL. The mass limiting current densities of both GDLs increased similarly by 210 mA/cm^2 as the air flow rate was increased from 2.1 to 4. Once again, the 10 wt.% GDL performs better at 0.6 V; however, the differences in the mass limiting current and the sensitivity to air flow rate between the two FEP contents diminish. As the under-humidified air promotes water removal from the GDL by evaporation and vapor phase diffusion, the level of liquid water saturation inside the GDL is reduced, resulting in a shrinking difference in the mass transport limiting behavior between 30 and 10 wt.% FEP-treated GDL.

Polarization behaviors of MEAs with MPL-coated 30 wt.%, no-MPL 30 wt.% and 10 wt.% FEP-impregnated cathode GDL were also measured at 90 °C in largely under-humidified condition, i.e. the humidifier temperature of 95 and 60 °C for hydrogen and air, respectively. Results are shown in Fig. 8. Interestingly, the MPL-coated GDL showed higher current densities in the kinetic regime, but a lower mass limiting current. This is likely because the additional resistance created by the presence of MPL protects the membrane from water loss to the dry gas in the kinetic regime while restricts oxygen transport in the mass transport control regime. Note also that the 10 wt.% FEP-GDL still showed higher performance throughout the entire voltage range than the 30 wt.% FEP-GDL.

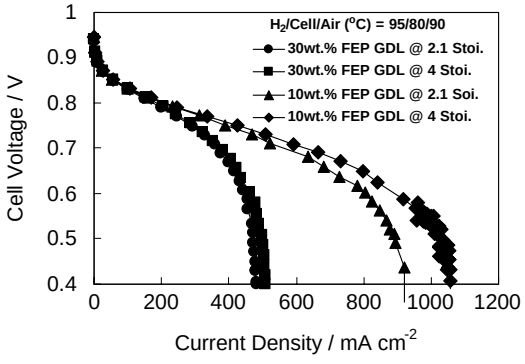

Fig. 6. Polarization curves obtained at 80 °C in 30 psi H_2/air from MEAs with two different FEP contents of cathode GDL under two different air stoichiometries (@ 1 A/cm^2 equivalent): (●) 30 wt.%-FEP cathode GDL and 2.1; (■) 30 wt.%-FEP cathode GDL and 4; (▲) 10 wt.%-FEP cathode GDL and 2.1; (◆) 10 wt.%-FEP cathode GDL and 4. Anode and cathode humidifier temperature was 95 and 90 °C, respectively. Pt loading was 0.22 mg/cm^2 at each electrode.

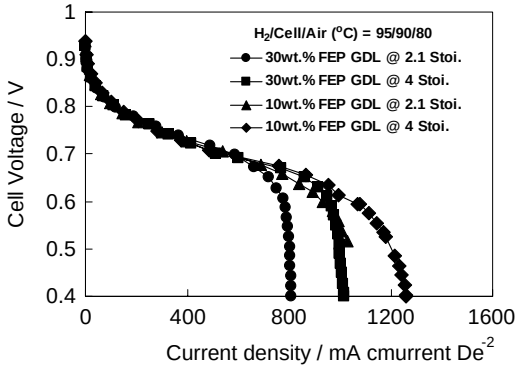

Fig. 7. Polarization curves obtained at 90 °C in 30 psi H_2/air from MEAs with two different FEP contents of cathode GDL under two different air stoichiometries (@ 1 A/cm^2 equivalent): (●) 30 wt.%-FEP cathode GDL and 2.1; (■) 30 wt.%-FEP cathode GDL and 4; (▲) 10 wt.%-FEP cathode GDL and 2.1; (◆) 10 wt.%-FEP cathode GDL and 4. Anode and cathode humidifier temperature was 95 and 80 °C, respectively. Pt loading was 0.22 mg/cm^2 at each electrode.

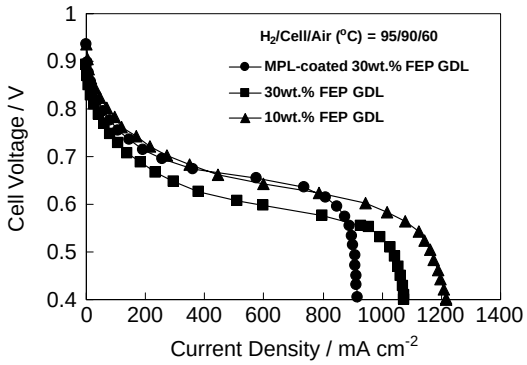

Fig. 8. Polarization curves obtained at 90 °C in 30 psi H_2/air from MEAs with three different types of cathode GDL under an air stoichiometry of 2.1 (@ 1 A/cm^2 equivalent): (●) microporous layer-coated and 30 wt.% FEP-impregnated GDL; (■) 30 wt.% FEP-impregnated GDL; (▲) 10 wt.% FEP-impregnated GDL. Anode and cathode humidification temperature was 95 and 60 °C, respectively.

As pointed out in the theoretical analysis of Wang [19], the mass transport limiting current is depending on GDL porosity, the level of liquid saturation inside the GDL, as well as the oxygen mass transfer coefficient at the GDL/channel interface. Based on this understanding and the results shown in Fig. 8, the 30 wt.% FEP GDL may have a lower porosity, mass transfer coefficient at the GDL/channel interface and hence higher liquid saturation inside the GDL.

Fig. 9 shows the effect of air flow rate on the polarization curves obtained at the cell temperature of 90 °C from MEAs of 30 and 10 wt.% FEP-GDL. The humidifier temperature of hydrogen and air was 95 and 60 °C, respectively. As expected, the increase of air flow rate resulted in higher mass limiting current. However, a significant voltage drop was observed in the kinetic regime as the air flow rate was increased, indicating membrane and catalyst layer dehydration under large flow rates of low-humidity air.

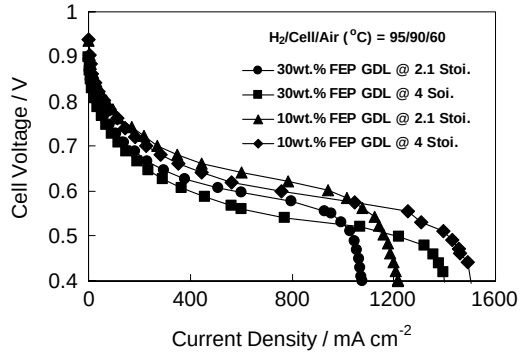

Fig. 9. Polarization curves obtained at 90 °C in 30 psi H_2/air from MEAs with two different FEP contents of cathode GDL under two different air stoichiometries (@ 1 A/cm^2 equivalent): (●) 30 wt.%-FEP cathode GDL and 2.1; (■) 30 wt.%-FEP cathode GDL and 4; (▲) 10 wt.%-FEP cathode GDL and 2.1; (◆) 10 wt.%-FEP cathode GDL and 4. Anode and cathode humidifier temperature was 95 and 60 °C, respectively. Pt loading was 0.22 mg/cm^2 at each electrode.

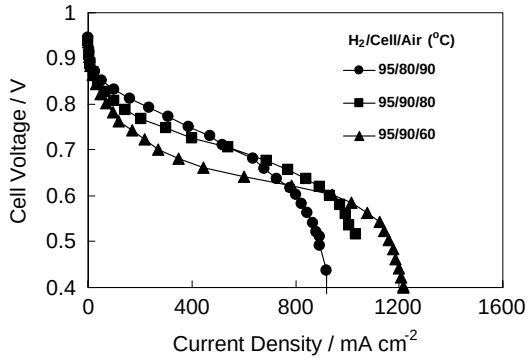

Fig. 10. Polarization curves obtained in 30 psi H_2/air from a MEA with 10 wt.% FEP-impregnated cathode GDL under an air stoichiometry of 2.1 (@ 1 A/cm^2 equivalent) at following humidification conditions (H_2/cell/air temperature): (●) 95/80/90 °C; (■) 95/90/80 °C; (▲) 95/90/60 °C.

The effect of the humidification condition on polarization curve of MEA with 10 wt.% FEP cathode is shown in Fig. 10. As the humidifier temperature of air was decreased, the mass transport limiting current density extended; however, the cell voltage in the kinetic regime decreased substantially under the constant flow rate. To better explain this observation, impedance spectra were taken at open-circuit under the various humidification conditions and the results are shown in Fig. 11. As the cathode humidity was decreased in the order of 95/80/90, 95/90/80 and 95/90/60 °C (hydrogen humidifier/cell/air humidifier temperature), the cell high-frequency resistance increased, indicating that ionomer in the cathode catalyst layer and also the membrane were dehydrated with decreasing humidification in the air stream. Although the high-frequency measurements were not carried out in the high current density range, it is expected that the membrane is re-hydrated by a large amount of water produced from the oxygen reduction reaction. This voltage loss in the kinetic-controlled regime under the low humidity condition has also been observed in Nafion 112 and 111 membranes, and is attributed to the potential drop in the electrolyte phase within the catalyst layer [21].

Power density versus current density curves for the MEA with 10 wt.% FEP-GDL obtained under different

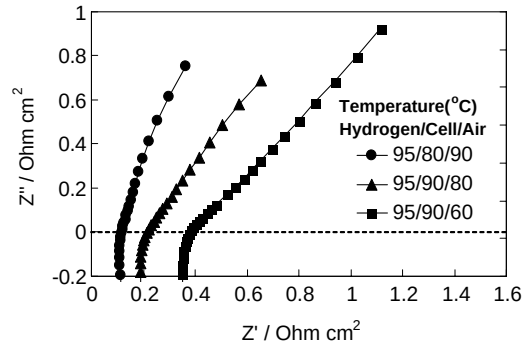

Fig. 11. Effect of humidification conditions on cell impedance measured at open-circuit, using 10 wt.% FEP-treated carbon paper as the cathode GDL and an air stoichiometry of 2.1 (@ 1 A/cm^2 equivalent).

humidification conditions and air flow rates are compared in Fig. 12. It is shown that the power performance varies strongly with the cathode humidification temperature and air flow rate. The peak power density increases with decreasing humidification temperature of cathode gas, trading off the power density losses in the kinetic regime with its gain in the ohmic and/or mass transport control regimes. As the humidifier temperature of air was decreased from 90 to 60 °C, the peak power increased from 0.48 to 0.6 W/cm^2, indicating that cathode flooding can be alleviated by using air feed of lower humidity. Under the same degree of low-cathode humidification, the power performance increased further from 0.6 to 0.7 W/cm^2 as the air stoichiometric flow rate was increased from 2.1 to 4.

Among possibilities responsible for the remarkable differences observed in power performance between 10 and 30 wt.% FEP-GDL, the hydrophobocity of the GDL is excluded since the contact angles measured from the two FEP contents were very similar as shown in Fig. 3. According to Bruggemann's equation, GDL porosity can also affect the mass transport rate through the GDL. The porosity change of carbon paper GDL due to FEP impregnation can be theoretically estimated under the assumption that FEP polymer distributes uniformly throughout the porous structure of GDL. As the hydrophobic polymer is impregnated into the carbon paper, its porosity decreases depending on the weight fraction of the hydrophobic polymer in the carbon paper according to

$$\varepsilon = \varepsilon_0 - \frac{V_{HP}}{V_{CP}} = \varepsilon_0 - \frac{x}{(1-x)}\frac{\rho_{CP}}{\rho_{HP}} \quad (2)$$

where ε is the porosity of wet-proof treated carbon paper, ε_0 the porosity of untreated carbon paper, V_{HP} the pore volume occupied by the hydrophobic polymer inside the carbon paper, V_{CP} the total volume of carbon paper, x the weight fraction of hydrophobic polymer in carbon paper, ρ_{CP} the density of carbon paper, and ρ_{HP} the density of hydrophobic polymer. Assuming that Toray paper bulk density is 0.49 g/cc [22], FEP density is 2.15 g/cc [23] and the porosity of untreated carbon paper is 0.8, the theoretical porosity of treated GDL containing 10, 20, 30, 40 wt.% of FEP was calculated to be 0.77, 0.74, 0.7, and 0.65, respectively. The change in bulk porosity due to FEP impregnation from 10 to 30 wt.% is thus only 0.07 and therefore is unlikely to cause the significant differences in cell polarization behaviors as observed in this work.

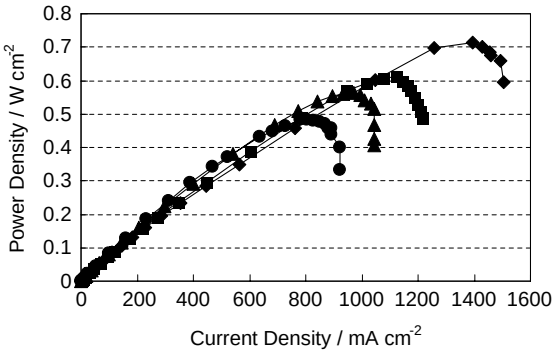

Fig. 12. Power density vs. current curve obtained in 30 psi H_2/air from MEAs with 10 wt.% FEP-treated cathode GDL at different humidification conditions (H_2/cell/air temperature) and air stoichiometries (@ 1 A/cm^2 equivalent): (●) 95/80/90 °C and 2.1; (▲) 95/90/80 °C and 2.1; (■) 95/90/60 °C and 2.1; (◆) 95/90/60 °C and 4.

The surface morphology of carbon paper impregnated with FEP was examined in order to find out a possible explanation for the difference in power performance. Fig. 13 shows the SEM micrographs for the GDLs untreated and treated with 20 wt.% FEP, respectively. Both GDLs are Toray paper, though not from the same lot. Interestingly, it appears that a significant number of pores near the surface, formed by multiple intersecting graphite fibers, were blocked by thin FEP films. Only large pores were kept open in the wet-proofed carbon paper. From this surface microstructure, it is inferred that the FEP hydrophobic polymer is localized more in the surface region than the interior. During the drying process after impregnation of FEP solution into carbon paper, the FEP solution inside the carbon paper must have migrated to the surface region, having higher drying rate, by

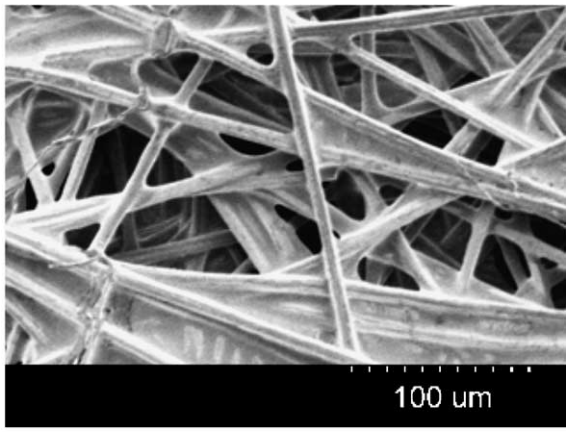

(a) 20 wt.% FEP carbon paper

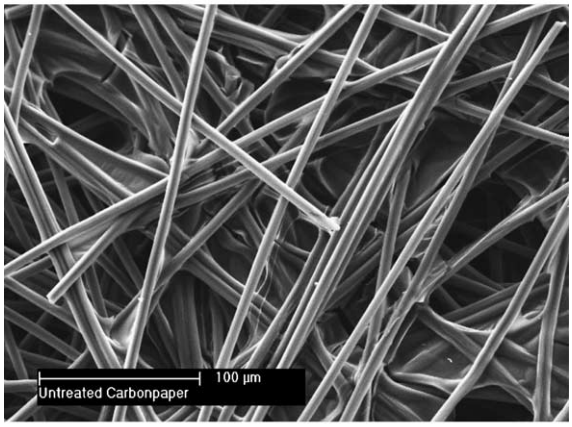

(b) untreated carbon paper

Fig. 13. Comparison of surface SEM micrographs of carbon paper impregnated with 20 wt.% FEP hydrophobic polymer to that untreated.

capillary force. Therefore, it is believed that the hydrophobic polymer is distributed more in the surface region of the carbon paper than in the bulk region, possibly reducing regional electrode porosity and modifying the surface pore structure of the carbon paper, appreciably.

The formation of a film of hydrophobic polymer blocking the pores near the surface was also observed [13] when the carbon paper was treated with a polytetrafluoroethylene suspension. It was reported that there exists an appreciable pressure drop across the GDL with increasing PTFE content. This interfacial modification, resulting from hydrophobic polymer impregnation, on both surfaces facing the gas channel and the catalyst layer, respectively, is believed to be the main reason behind the difference in polarization behavior.

In summary, it appears that 10 wt.% FEP loading is sufficient to result in a hydrophobic surface to facilitate liquid water removal, and that higher FEP content in excess of 10 wt.% can only block GDL surface pores, thus imposing significant mass transport limitations due to both oxygen transport and water removal through a highly restricted GDL surface.

4. Conclusion

Effects of FEP hydrophobic polymer content in carbon paper GDL on the power performance of H_2/air PEM fuel cells have been studied and characterized comprehensively. The contact angle measurements indicated a similar level of hydrophobicity among GDLs impregnated with different amounts of FEP ranging from 10 to 40 wt.%. The contact angle was found to be a strong function of temperature, with the value close to 80° at the water temperature of 80 °C. The single cell tests under various cathode humidification and flow rate conditions, however, reveal that the MEA with 10 wt.% FEP-impregnated cathode GDL provided much higher power densities than the one with 30 wt.% FEP-impregnated carbon paper. It was concluded that this substantial difference in power performance originates primarily from the surface modification due to the fact that excessive FEP impregnation results in significant blockage of surface pores by thin FEP films and hence a highly restricted surface for reactant transport and product removal. The present study clearly suggests that 10 wt.% FEP loading in GDL is sufficient to create hydrophobicity for easy removal of liquid water and at the same time leaves the GDL surface relatively accessible for the reactant and product moving in and out.

Acknowledgements

Funding for this work from DOE ultra-clean fuel program under cooperative agreement no. DE-FC26-01NT41098 is acknowledged. Partial support from Toyota Motor Corporation is also acknowledged.

References

[1] M.S. Wilson, S. Gottesfeld, J. Appl. Electrochem. 22 (1992) 1.
[2] M.S. Wilson, S. Gottesfeld, J. Electrochem. Soc. 139 (1992) L28.
[3] M.S. Wilson, J.A. Valerio, S. Gottesfeld, Electrochim. Acta 40 (1995) 355.
[4] M.S. Wilson, T.E. Springer, J.R. Davey, S. Gottesfeld, in: S. Gottesfeld, G. Halpert, A. Landgrebe (Eds.), Proceedings of the First International Symposium on Proton Conducting Membrane Fuel Cells I, PV95-23, The Electrochemical Society, 1995, p. 115.
[5] E. Antolini, R.R. Passor, E.A. Ticianelli, J. Power Sources 109 (2002) 477.
[6] T. Ralph, G. Hards, J. Keating, J. Electrochem. Soc. 144 (1997) 3845.
[7] E. Passalacqua, F. Lufrano, G. Squadrito, A. Patti, L. Giorgi, Electrochim. Acta 43 (1998) 3665.
[8] L. Giorgi, E. Antolini, A. Pozio, E. Passalacqua, Electrochim. Acta 43 (1998) 3675.
[9] J.R. Jordan, A.K. Shukla, T. Behrsing, N.R. Avery, B.C. Muddle, M. Forsyth, J. Appl. Electrochem. 30 (2000) 641.
[10] J.R. Jordan, A.K. Shukla, T. Behrsing, N.R. Avery, B.C. Muddle, M. Forsyth, J. Power Sources 86 (2000) 250.
[11] E. Passalacqua, G. Squadrito, F. Lufrano, A. Patti, L. Giorgi, J. Appl. Electrochem. 31 (2001) 449.
[12] D.S. Chan, C.C. Wan, J. Power Sources 50 (1994) 163.
[13] D. Bevers, R. Rogers, M. Bradke, J. Power Sources 63 (1996) 193.
[14] S. Swathirajan, et al., US Patent 6,277,513B1 (August) (2001).
[15] C. Lim, C.Y. Wang, J. Power Sources 113 (2003) 145.
[16] D. Weng, J.S. Wainright, U. Landau, R.F. Savinell, J. Electrochem. Soc. 143 (1996) 1260.
[17] J.B. Cain, D.W. Francis, R.D. Venter, A.W. Neumann, J. Colloid Interface Sci. 94 (1983) 123.
[18] A.W. Neumann, Z. Physik Chem. Neve. Folge. 41 (1964) 339.
[19] C.Y. Wang, in: W. Vielstich, A. Lamm, H. Gasteiger (Eds.), Handbook of Fuel Cells, vol. 3, Wiley and Sons Ltd., 2003, Chapter 29, p. 337.
[20] U. Pasaogullari, C.Y. Wang, J. Electrochem. Soc. 151 (2004) A399.
[21] H.A. Gasteiger, W. Gu, R. Makharia, M.F. Mathias, B. Sompalli, in: W. Vielstich, H.A. Gasteiger, A. Lamm (Eds.), Handbook of Fuel Cells-Fundamentals, Technology and Applications, vol. 3, John Wiley & Sons Ltd., 2003, Chapter 46, p. 593.
[22] Product Specifications, in: http://www.etek-inc.com.
[23] Specification Bulletin, No. H-55003-2, Dupont.